$BaTiO_3/CoFe_2O_4$ particulate composites with large high frequency magnetoelectric response

S. Q. REN, L. Q. WENG*, S.-H. SONG, F. LI
Department of Materials Science and Engineering, Shenzhen Graduate School, Harbin Institute of Technology, Shenzhen University Town, Xili, Shenzhen 518055, People's Republic of China
E-mail: lqweng@hitsz.edu.cn

J. G. WAN, M. ZENG
Laboratory of Solid State Microstructures, Nanjing University, Nanjing 210093, People's Republic of China

The multiferroic composites consisting of piezoelectric and piezomagnetic component phases show a magnetoelectric coupling effect (ME) due to the magnetically or electrically induced mechanical deformation between these two phases [1]. To the magnetic field induced ME effect, the applied magnetic field generates a strain in piezomagnetic phase that deforms piezoelectric phase. As a result, the deformation of piezoelectric phase produces an electric field. Similarly the electrical field induced ME effect can be realized by applying an electric field. The ME effect occurs as a product property between piezoelectric and piezomagnetic phases and is not available in their individual component phases. ME voltage coefficient α^E is adopted to measure the magnetic field induced ME effect as follows

$$\alpha^E = \frac{\partial e}{\partial H} \times \frac{\partial E}{\partial e} \quad (1)$$

where e is elastic strain, H is applied magnetic field and E is induced electric field. The direction of the generated electrical field is apparently determined by the orientation of the Weiss domains (groups of dipoles with parallel orientation) in the piezoelectric phase that is random before poling. Thus, the alignment of the electric dipoles, usually realized by the poling process, is essential in order to achieve substantial ME effect. Studies by Van den Boomgaard *et al.* [2–4] have first demonstrated that the effective magnetoelectric coupling effect in the composite materials relies on optimal composition, favorable microstructure and non-slip contact between different phases.

Among various magnetoelectric composite systems, $BaTiO_3/CoFe_2O_4$ composite materials are the first investigated [2–4]. The $BaTiO_3$ and $CoFe_2O_4$ phases are found to be separated from each other by cooling the eutectic liquid in a unidirectional solidification process, which produces the $BaTiO_3/CoFe_2O_4$ composites with a lamellar morphology. However, the phases as Co_2TiO_4 and $(BaFe_{12}O_{19})_y(BaCo_6Ti_6O_{19})_{1-y}$ could also exist in the systems [4]. The resulting lamellar microstructure prevents the relatively conductive $CoFe_2O_4$ phase from forming conducting chains along the poling direction. Consequently the composite materials possess a relatively high ME sensitivity (130 mV/cm·Oe), but the unidirectional solidification process is not easy to be implemented. Moreover, a recent study by Echigoya *et al.* [5] demonstrates that it is difficult to obtain an ideal lamellar microstructure of the as-produced composite materials, and thus their electrical resistivity is limited to about 10^8 Ω·cm, which is not high enough for applying higher poling voltage. The occurrence of $BaTiO_3$ and $CoFe_2O_4$ phase separation has also been observed, according to Ramesh *et al.* [6], through cooling an atomic gaseous phase in the sputtering process that gives a self-assembled nanostructure. Nevertheless, the phase separation or segregation has not ever been observed from solid state precursors in the $BaTiO_3/CoFe_2O_4$ system. Hence many studies [7–10] have adopted conventional ceramic processes to produce the composites by mixing and sintering $BaTiO_3$ and $CoFe_2O_4$ powders together. The magnetoelectric sensitivity of these materials was usually poor due to the undesirable $CoFe_2O_4$ phase distribution and the lack of control to the microstructure of the composites. To overcome these difficulties, this letter reports a novel approach of preparing multiferroic $BaTiO_3/CoFe_2O_4$ composites through a one-pot process.

The one-pot process was employed as follows to prepare stoichiometric $BaTiO_3/CoFe_2O_4$ (molar ratio: 4:1) powder. The starting materials were reagent grade $Ba(NO_3)_2$(>99%), butyl titanate $Ti(OC_4H_9)_4$(>99%), $Co(NO_3)_2$ and $Fe(NO_3)_3$. 0.1 mol $Ba(NO_3)_2$ was first dissolved in 500 ml distilled water and the solution was then gradually added to 500 ml 0.2 M ethylenediaminetetraacetic acid (EDTA) solution with pH 6 adjusted by adding an ammonia solution. Similarly Co and Fe ion-containing solutions stabilized by EDTA were prepared. The stoichiometric amount of butyl titanate was added to a 0.2 M citric acid solution (pH 6) with the molar ratio of $Ti(OC_4H_9)_4$ to citric acid being 1:2. The solutions containing Ba, Co, Fe and Ti components were then mixed by mechanical stirring at 70 °C until a viscous liquid appeared. Water in the liquid was removed in oven at 120 °C. The dried mixture was heat-treated at various temperatures for 1 hr to investigate its phase development. The calcined powder was ball milled for 4 hr in a plenary mill before

---

*Author to whom all correspondence should be addressed.

0022–2461

uniaxially pressed into disc-shaped samples. The nominal size of the samples is 10 mm in diameter and 1 mm in thickness. The samples were sintered at different temperatures in air for a holding time of 2 hr with a heating rate of 2 °C/min. Differential thermal analysis (DTA) and thermogravimetry (TG) (Perkin Elmer 1700) were carried out to monitor the decomposition process of the precursor at a heating rate of 5 °C/min in static air. Crystal structure changes of the samples after heat treatment were identified by X-ray diffraction (XRD, D8 ADVANCE, Bruker) with CuKa radiation. Microstructural and compositional observations of the polished and Pt-coated sections of the sintered samples were performed by scanning electron microscopy (SEM, Jeol, JSM-5610LV) equipped with energy dispersive X-ray spectroscopy (EDS).

The electric resistivity of the sintered samples was measured between room temperature and 150 °C by a digital multimeter. Then these samples were electrically polarized under 1 kV/mm at 140 °C to align the electric dipoles in the piezoelectric $BaTiO_3$ phase. The ME response was measured under a dc magnetic field up to 0.4 T and a superimposed ac magnetic signal of less than 5 Oe amplitude. Both the ac magnetic field and the magnetic bias are parallel to the poling direction of the samples. The frequency dependence of the ME sensitivity of the samples was measured and it was found that the ME reached a maximum at about 160 kHz, suggesting that the electromechanical resonance achieved at this frequency. The peak ME response is attributed to the enhanced coupling elastic interaction between $BaTiO_3$ and $CoFe_2O_4$ phases [11].

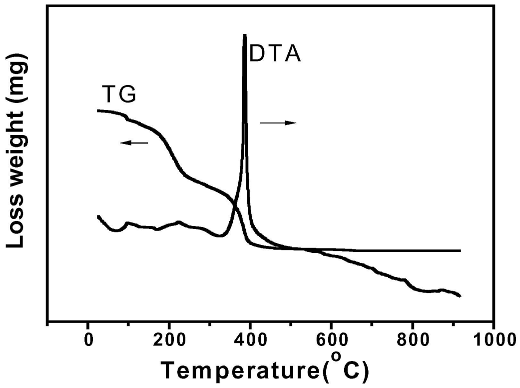

Figure 1 DTA and TG results of the precursor heat-treated at a heating rate of 5 °C/min in static air.

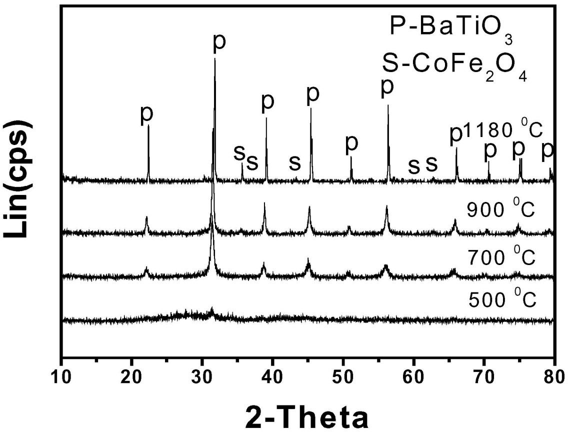

Figure 2 XRD patterns of the samples with a composition of 0.8 $BaTiO_3$·0.2 $CoFe_2O_4$, heat-treated at 500 °C, 700 °C, 900 °C and 1180 °C respectively.

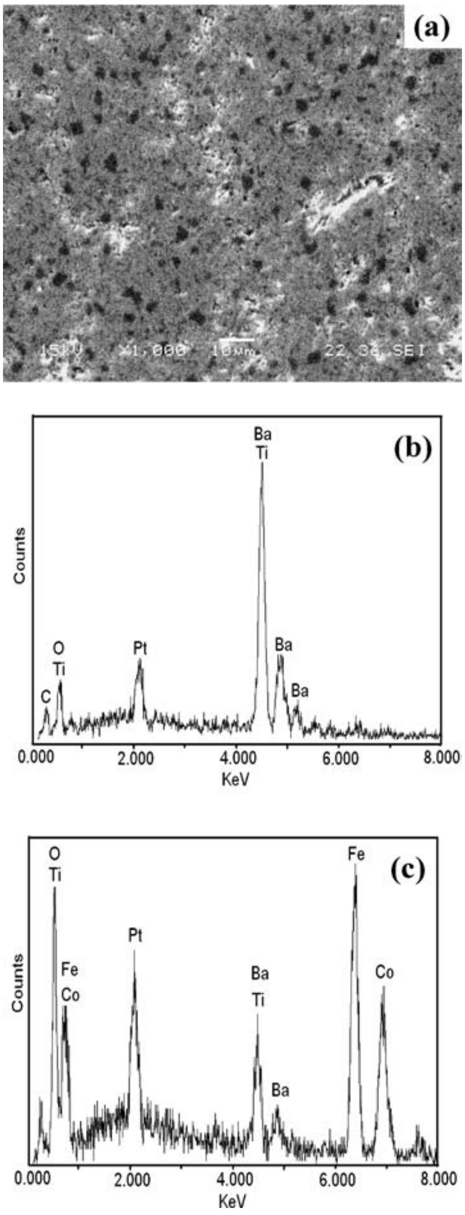

Figure 3 (a) Typical SEM micrograph of the polished surface of the composite samples sintered at 1180 °C for 2 hr, and EDS spectra of (b) matrix phase and (c) the phase in black.

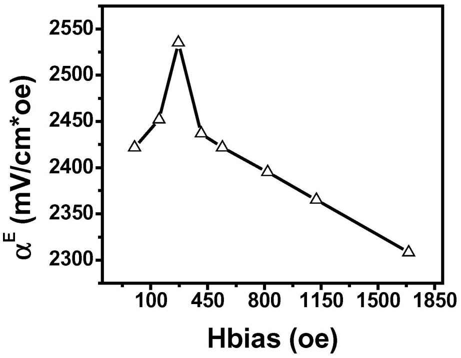

Figure 4 Magnetoelectric voltage coefficient as a function of d.c magnetic bias field for the composite samples sintered at 1180 °C for 2 hr.

The excellent compositional homogeneity of perovskite gel precursors complexed by EDTA and citric

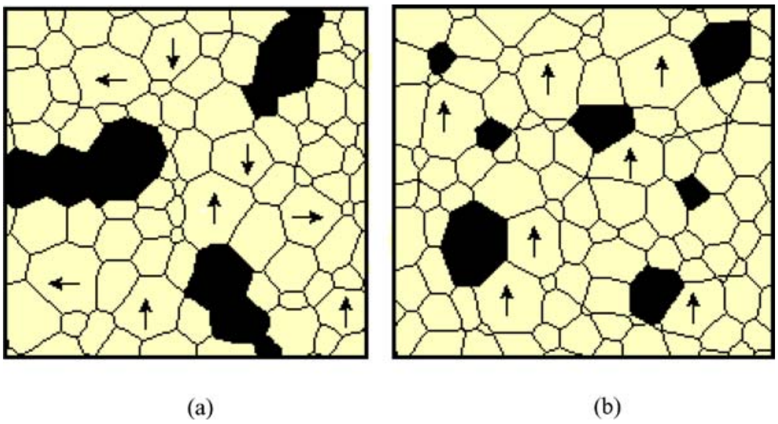

Figure 5 Schematic diagrams of distribution of $CoFe_2O_4$ phase (in black) in $BaTiO_3$ matrix (in grey) in two different ways. (a) composite materials prepared by mixing and sintering method, (b) composite materials produced by one-pot approach in the present study.

acid has been well studied with confirmatory supporting evidences from Sale [12] and Hodgson *et al.* [13]. In the present study, the dried gel containing Ba, Ti, Co and Fe components is completely decomposed to give inorganic precursor at about 500 °C since, as shown in the thermogravimetry (TG) curve (Fig. 1), there is no further weight loss above this temperature. Therefore, the thermal effects of DTA curve (Fig. 1) can be attributed to the phase transformation above 500 °C, which is supported by the XRD (Fig. 2). The XRD shows that the precursor is amorphous at 500 °C (Fig. 2). With further increasing temperature to 700 °C, the crystalline $BaTiO_3$ phase is formed but the $CoFe_2O_4$ phase cannot be identified until 900 °C. The XRD patterns of the sample heat-treated at 1180 °C are assigned only to both $BaTiO_3$ and $CoFe_2O_4$ phases and no other phases are present. These results indicate that the $BaTiO_3$ and $CoFe_2O_4$ phases segregate each other from an initially amorphous solid phase. SEM observations (Fig. 3a) show that a phase in black is evenly embedded in the matrix in an isolated and particulate manner. The EDS results (Fig. 3b) of the matrix show strong Ba and Ti peaks with little appearance of Co and Fe peaks, suggesting that the composition of the matrix is $BaTiO_3$. On the other hand, the phase in black is identified as $CoFe_2O_4$ since EDS (Fig. 3c) exhibits strong Co and Fe peaks. Although the Ba and Ti peaks also appear in Fig. 3c, they probably result from the $BaTiO_3$ matrix beneath the $CoFe_2O_4$ particulate phase since the incident electron beam could penetrate several micrometers in depth in the sample. Furthermore, XRD results (Fig. 2) have confirmed the $CoFe_2O_4$ existing in the matrix as a pure and single phase.

Fig. 4 shows the ME sensitivity variation as a function of the dc magnetic bias. The magnetoelectric voltage coefficient, α^E, initially increases with the bias field and then saturates at about 0.27 kOe with the maximum ME sensitivity reaching 2540 mV/cm·Oe. Further increasing the bias field results in a decrease in magnetoelectric voltage coefficient, according to Equation 1, since the induced electric field has been saturated. This trend of the ME sensitivity variation as a function of the dc magnetic bias is consistent with previous studies [14–16]. However, the magnetoelectric effect at high frequencies, comparable to those observed for the PZT/ferrite laminated composites [8], is much higher than that observed in the $BaTiO_3/CoFe_2O_4$ particulate composite systems reported in the literature[3, 16]. This may be due to the much improved distribution of $CoFe_2O_4$ phase in the $BaTiO_3$ matrix. As shown in Fig. 5, the $BaTiO_3/CoFe_2O_4$ particulate composite systems prepared by mixing and sintering $BaTiO_3$ and $CoFe_2O_4$ powders inevitably form aggregates with irregular morphology, which act as the conductive channels to disable the poling effort. Therefore, the electric dipoles in the $BaTiO_3$ matrix remain largely unaligned (Fig. 5a). In contrast, the $BaTiO_3/CoFe_2O_4$ particulate composite systems produced in the present study have an electrical resistivity over 10^{11} $\Omega\cdot$ cm between room temperature and 150 °C, which is significantly higher than the reported values in the literature [5]. The high electrical resistivity is, as schematically shown in Fig. 5b, due to the homogeneous distribution of $CoFe_2O_4$ particulates in the $BaTiO_3$ matrix where $CoFe_2O_4$ particulates are isolated. Therefore, the effective poling can be implemented, leading to the electric dipoles in the $BaTiO_3$ matrix staying roughly in alignment (Fig. 5b). As a result, the ME effect is much enhanced.

In conclusion, the $BaTiO_3/CoFe_2O_4$ particulate composites are synthesized by a one-pot process. Particulate $CoFe_2O_4$ phase is embedded in the $BaTiO_3$ matrix homogeneously with 3-0 connectivity via a phase segregation mechanism, leading to an excellent interface contact between the $BaTiO_3/CoFe_2O_4$ phases and the high insulation. Consequently, the particulate composite exhibits high ME sensitivity, and the maximum α_E at the optimal magnetic bias of 0.27 kOe reaches 2540 mV/cm·Oe at 160 kHz, comparable to the lead-zirconate titanate (PZT)/polyvinylidene-fluoride (PVDF) and Tb–Dy–Fe alloy (Terfenol-D) particulate composite layers [17].

References

1. V. M. LALETIN, *Sov. Tech. Phys. Lett.* **17** (1991) 1342.
2. J. V. D. BOOMGAARD and R. A. J. BORN, *J. Mater. Sci.* **13** (1978) 1538.
3. J. V. D. BOOMGAARD, A. M. J. G. VANRUN and J. V. SUCHTELEN, *Ferroelectrics* **10** (1976) 295.
4. *Idem., ibid.* **14** (1976) 727.

5. J. ECHIGOYA, S. HAYASHI and Y. OBI, *J. Mater. Sci.* **35** (2000) 5587.
6. H. ZHENG, J. WANG, S. E. LOFLAND, Z. MA, L. MOHADDES-ARDABILI, T. ZHAO, F. BAI, L. SALAMANCERIBA, S. R. SHINDE, S. B. OGALE, D. VIEHLAND, Y. JIA, D. G. SCHLOM, M. WUTTIG, A. ROYTBURG and R. RAMESH, *Science.* **303** (2004) 661.
7. M. AVELLANEDA and G. HARSHE, *J. Intel. Mater. Syst. Struct.* **5** (1994) 501.
8. G. SRINIVASAN, E. T. RASMUSSEN, J. GALLEGOS, R. SRINIVASAN, I. YU, I. BOKHAN and V. M.LALEIN, *Phys. Rev. B* **64** (2001) 214408.
9. S. LOPATIN, I. LOPATINA and I. LISNEVSKAYA, *Ferroelectrics* **162** (1994) 63.
10. C. W. NAN, *Phys. Rev. B.* **50** (1994) 6082.
11. N. CAI, C. W. NAN, J. ZHAI and Y. LIN, *Appl. Phys. Lett.* **84** (2004) 3516.
12. H. W. WANG, D. HALL and F. SALE, *J. Am. Ceram. Soc.* **75** (1992) 124.
13. S. N. B. HODGSON and X. SHEN, *J. Mater. Sci.* **35** (2000) 5275.
14. M. I. BICHURIN, D. A. FILIPPOV, V. M. PETROV, V. M. LALETIN, N. PADDUBNAYA and G. SRINIVASAN, *Phys. Rev. B.* **68** (2003) 132408.
15. N. CAI, J. ZHAI, C.-W. NAN, Y. LIN and Z. SHI, *Phys. Rev. B.* **68** (2003) 224103.
16. K. K. PATANKAR and P. D. DOMBALE, *J. Electroceram.* **6** (2001)115.
17. C. W. NAN, L. LIN, N. CAI, J. ZHAI, Y. YE, Y. H. LIN, L. J. DONG and C. X. XIONG, *Appl. Phys. Lett.* **81** (2002) 3811.

Received 24 November 2004
and accepted 22 February 2005